Rare Metal Materials and Engineering
Volume 49, Issue 6, June 2020
Available online at www.rmme.ac.cn

Science Press

Cite this article as: Rare Metal Materials and Engineering, 2020, 49(6): 1925-1930.

ARTICLE

Microstructure and Properties of γ-TiAl Alloy Fabricated by Laser Melting Deposition

Liu Zhanqi, Wang Wenbo, Ma Ruixin, Xu Guojian, Zheng Wentao

Shenyang University of Technology, Shenyang 110870, China

Abstract: The deposited sample of $X\times Y\times Z$ (40 mm×5 mm×60 mm) Ti-48Al-2Cr-2Nb alloy was fabricated by laser melting deposition. The microstructure, phase composition, grain orientation and fracture morphology of the deposited sample were analyzed by optical microscope (OM), scanning electron microscope (SEM), X-ray diffraction (XRD), transmission electron microscope (TEM) and electron backscattering diffraction (EBSD). The hardness distribution at different positions of the deposited sample was measured by Vickers hardness tester. The tensile properties of the deposited sample in Z direction were measured by tensile machine. The results show that the well-formed deposited sample is obtained under the optimum process parameters, and no surface cracks are found after penetration detection. The microstructure of the deposited sample is composed of $\alpha_2+\gamma$ lamellar colony and a small amount of bulk γ phase. For as-deposited γ-TiAl alloy, the room-temperature tensile strength along the Z direction is 425 MPa and the elongation is 3.3%. The fracture morphology of tensile specimen is quasi-cleavage fracture.

Key words: laser melting deposition; γ-TiAl alloy; microstructure; mechanical properties

TiAl alloys have high melting point (>1450 °C), low density (up to 4 g/cm^3), high elastic modulus (160~180 GPa) and high creep strength (up to 900 °C). In recent years, TiAl alloys have gradually replaced titanium alloys, nickel-based superalloys and heat-resistant steels, and have great potential in aerospace and vehicle engine manufacturing[1-3].

TiAl alloys have poor plasticity and ductility at room temperature, so it is difficult to process them by conventional manufacturing process, which limits the wide application of TiAl alloys[4]. Existing titanium alloy forming methods are mainly near-net forming, including powder metallurgy, precision manufacturing and directional solidification. The laser coaxial powder feeding technology has obvious advantages in near-net forming of TiAl alloy. In addition, under the action of laser beam, the microstructure and properties of materials can be controlled effectively by optimizing the process parameters, and the density of the microstructure can reach above 98.5%[5].

At present, TiAl alloys have been prepared by laser melting deposition (LMD) technology, and the microstructure and properties of TiAl alloys have been studied. Ti-48Al-2Cr-2Nb alloy was prepared by Jan Schwerdtfeger et al[6], and its microstructure was refined by adjusting the beam parameters. Qu et al[7] investigated Ti-47Al-2.5V-1Cr alloy thin-walled part with oriented columnar grains, and the samples were prepared by LMD technique, and the microstructure and tensile properties at room temperature were analyzed. Zhang et al[8] 's testings show that the substrate has significant effect on the microstructure of the deposited layer, and ultrafine lamellar microstructure is obtained by controlled post-heat treatment, but the microstructure difference and grain orientation of each part of the thin-walled part have not been analyzed and explained.

In this paper, Ti-48Al-2Cr-2Nb alloy powder was studied. The microstructure and properties of deposited sample were analyzed, which provides the experimental foundation for aerospace printing high temperature blades.

1 Experiment

The experiment used powder material was Ti-48Al-2Cr-2Nb

Received date: June 18, 2019
Foundation item: Intelligent Additive Manufacturing System Platform (2017YFB1103000)
Corresponding author: Xu Guojian, Ph. D., Professor, School of Materials Science and Engineering, Shenyang University of Technology, Shenyang 110870, P. R. China, Tel: 0086-24-25496302, E-mail: xuguojian1959@qq.com

alloy (particle size 53~150 um), and chemical composition (wt%) of Ti-48Al-2Cr-2Nb alloy powder was Al 32.5, Cr 2.64, Nb 4.62, O 0.06, N 0.005, and balance Ti. The alloy powder was dried at 150 °C for 1.5 h. An adopted substrate was TC4 titanium alloy, the size of which is 100 mm×100 mm×20 mm. A grinder and acetone were used to remove impurities such as oxide film and oil on the substrate surface.

LDM8060 laser equipment produced by RAYCHAM was used in the experiment. The laser type was LDF4000-100 semiconductor laser (rated output power 4 kW, transmission fiber core diameter 1000 μm). The technological parameters in the experiment process are as follows: laser power 1400 W, scanning speed 9 mm/s, powder feeding speed 5.67 g/min, laser spot diameter 3 mm, defocus amount 0 mm, powder feeding gas (Ar) flow rate 8 L/min, substrate preheating temperature 350 °C, its protective gas of sealed working chamber was 99.99% Ar, and the water and oxygen content in sealed working chamber ≤50 μg/g.

The deposited sample was cut into 10 mm× 5 mm× 60 mm blocks for microstructure observation. Then they were ground with sandpaper (800#, 1000#, 1500#, 2000# in order of size), and polished with ET-500 environment-friendly diamond spray polishing agent (particle size: 2.5, 1.5, 0.5 μm, respectively. The corrosion solution was Kroll solution (HF: HNO_3:H_2O=2:3:10, volume ratio), and the corrosion time was about 15 s. After corrosion, the sample was washed with alcohol and dried by air dryer. The microstructure of the deposited layer was analyzed by ZX-10 Zeiss microscope (OM) and Hitachi S-3400N and SU8010N field emission scanning electron microscope (SEM). The phase composition of the deposited layer was analyzed by X-7000 X-ray diffraction analyzer. Microstructure morphology was observed by JEM-2100 transmission electron microscope. The phase distribution and grain orientation in the microstructure were analyzed by EBSD with Gemini SEM300 field emission scanning electron microscope. The dimension of the tensile specimen is shown in Fig.1. The processed tensile part was put into a SLFL-100KN tensile machine for room temperature tensile testing at a loading rate of 0.3 mm/min. The fracture morphology of tensile specimen was observed by scanning electron microscope (SEM). The distribution of Vickers hardness (load 1.96 N, duration 10 s) was measured by Vickers hardness tester.

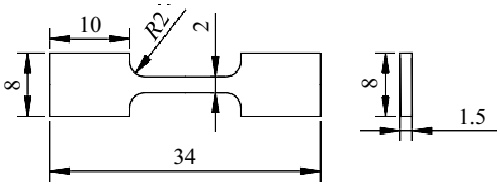

Fig.1 Drawing of tensile specimen size

2 Results and Discussion

2.1 Appearance of the deposited sample

The defect-free deposited sample with size of 40 mm×5 mm ×60 mm was fabricated. The specific printing process is that each layer is 0.4 mm thick and 150 layers are printed. During the printing process, for every 10 layers printed, there is a waiting time of 10 s. In order to prevent the deposited sample from collapsing due to excessive energy input, the process is repeated until the printing is finished. No surface cracks was found on the surface of the formed deposited sample through penetration testing analysis, as shown in Fig.2.

2.2 Microstructure of deposited sample

The deposited sample was prepared by using the optimum process parameters. The optical microstructure of the deposited sample is shown in Fig.3. As can be seen from Fig.3, the macro-structure of the deposited sample is composed of single channel multi-layer, and the obvious layer-band structure appears between layers. In addition, coarser columnar crystals can penetrate multiple deposited layers. This is because the lower surface is partially remelted when the upper layer is

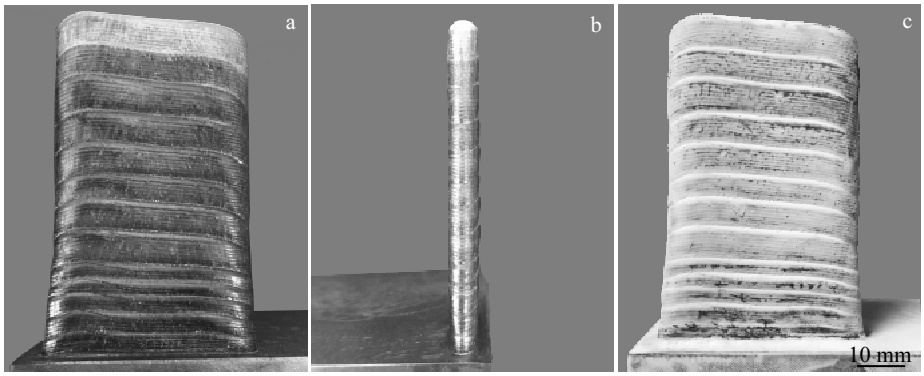

Fig.2 Appearance morphologies and non-destructive testing results of deposited sample: (a) *X-Z* face, (b) *Y-Z* face, and (c) non-destructive testing face

deposited, and the opposite heat dissipation rate of the deposition direction is the fastest in the subsequent cooling process, so that the molten pool metal nucleates and grows as epitaxial crystals, resulting in coarse columnar crystals growing along the deposited direction and traversing several deposited layers[9,10].

In order to further analyze the microstructure, the three areas of A, B and C in Fig.3a, 3b and 3c are enlarged respectively, and the enlarged microstructure corresponds to Fig. 3d, 3e and 3f, respectively. From the Fig.3, we can see that its microstructure is composed of lamellar clusters.

A small number of microcracks can be observed in the microstructure of Fig.3d, and the cracks are mainly concentrated at the top of the deposited sample. However, no microcracks are found in Fig.3e and 3f. In Fig.3d, the main cause of micro-crack formation is that there is no heat input at the end of the deposited sample, resulting in too fast cooling rate and excessive thermal stress, which eventually leads to the formation of microcracks at the top of the deposited sample.

In addition, the microstructure was further enlarged by SEM and TEM analysis as shown in Fig.4. And the structure is clearer than that of the optical microstructure. From the results of the X-ray diffraction analysis of Fig.5 and the EBSD phase analysis of Fig.6, it is determined that the lamellar structure in Fig.4a (SEM) and 4b (TEM) morphology is composed of γ-TiAl+α_2-Ti_3Al phases. As can be seen from Fig.5, the X-ray diffraction peak on the (401) plane near the substrate is higher than that on the intermediate layer and the top layer. The results show that the content of α_2 phase near the substrate is more than that in other regions. In the vicinity of the substrate, because of the dilution effect of TC4 base metal on γ-TiAl alloy, the content of Ti element in the deposited sample relatively increases, which leads to the relative decrease of Al element content. Therefore, it is inferred that the increase of α_2 phase near the substrate is caused by the dilution effect of TC4 substrate.

As shown in Fig.6a, the phase content of γ-TiAl and α_2-Ti_3Al is 96.7% and 3.3%, respectively. Fig.6b is a reverse pole diagram representing the relationship between color and crystal orientation in the EBSD picture[11,12]. The orientation of the pink block γ phase in Fig.6c is substantially the same as that of the lamellar γ phase. As can be seen from Fig.6c and 6d, in lamellar microstructure, lamellar α_2 phases generally precipitate along lamellar γ subgrain boundaries, both of which maintain Blackburn coherence[13,14].

2.3 Hardness of deposited sample

A schematic diagram of the Vickers hardness testing points and results of the deposited sample are shown in Fig.7 and Fig.8, respectively. As can be seen from Fig.8a, the testing method is to take the first deposited layer as the testing zero point, test one point every 0.5 mm from bottom to top, test three hardness values at each point, and take the average value. As can be seen from Fig.8b, the testing method is to take the center as the testing zero point, have the center to both sides, test one point every 0.5 mm, test three hardness values at each point, and take the average value. Detailed measurements are shown in Fig.8.

The distribution range of Vickers hardness is 3300~4500 MPa. During the deposition of the first layer, due to the dilution effect of TC4 substrate on γ-TiAl alloy, the content of Ti element in the deposited layer relatively increases, which leads to the relative decrease of Al element content, so the

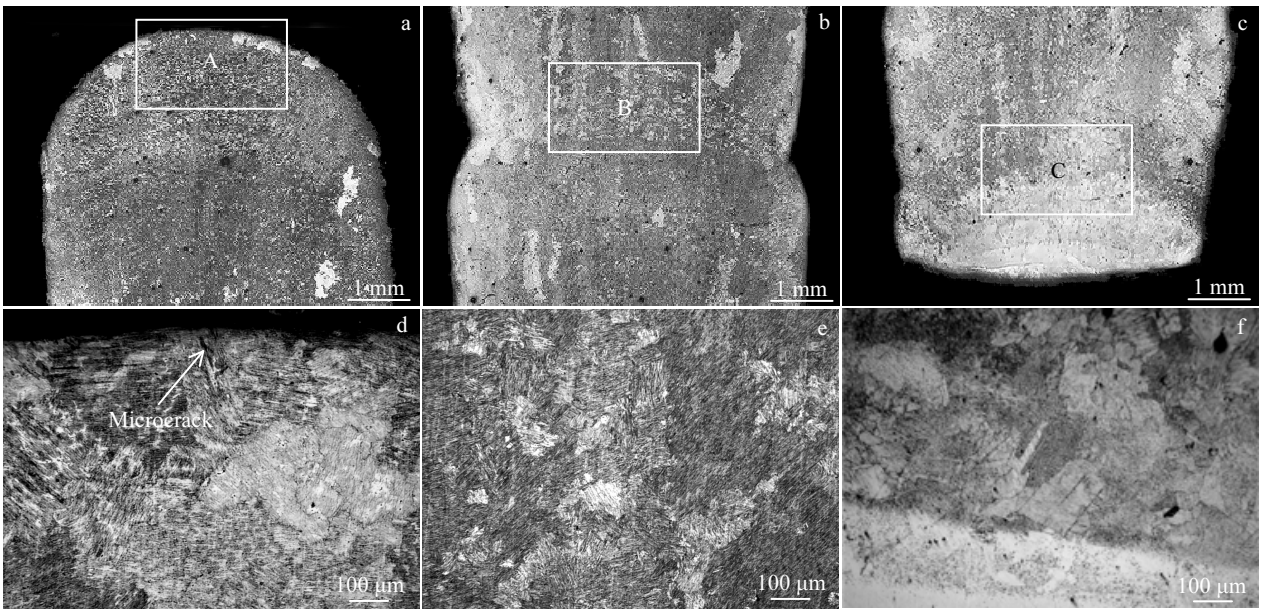

Fig.3 Optical microstructures of deposited sample of macro structure of the top region (a, d); the middle region (b,e); the bottom region (c, f)

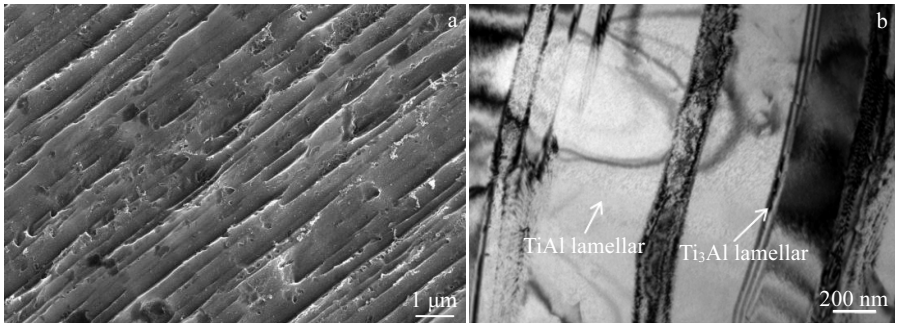

Fig.4 SEM image (a) and TEM image (b) of microstructure in the middle region of the deposited layer

content of α_2 phase in the deposited layer near the substrate is also higher, which is caused by the dilution effect of TC4 substrate on γ-TiAl alloy. In addition, because the cooling rate is faster in the deposition state, the alloying elements cannot diffuse and form martensite structure in time, so the hardness value increases with the increase of α_2 phase content[15]. The hardness of the deposited layer is about 3550 MPa because the dilution effect of the substrate on the deposited layer disappears when the deposited layers are more than three layers.

2.4 Properties of deposited sample

The related research on the crack problem of TiAl alloy shows that the main causes of material cracking are high temperature gradient and thermal stress. The solution to the crack problem is mainly to preheat the substrate, which can reduce the temperature gradient and thermal stress. Zhang et al[9] have tested mechanical properties of Ti-47Al-2Cr-2Nb-0.5W-0.15B materials. At room temperature, the tensile strength in *XY* and *Z* direction are 810 and 575 MPa, respectively.

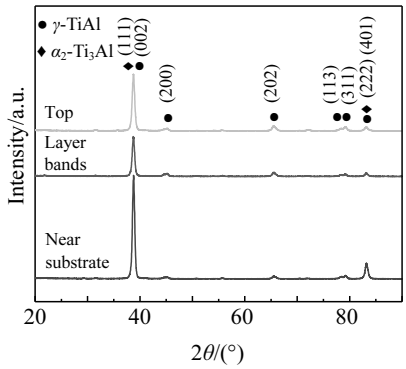

Fig.5 X-ray diffraction patterns of deposited layer

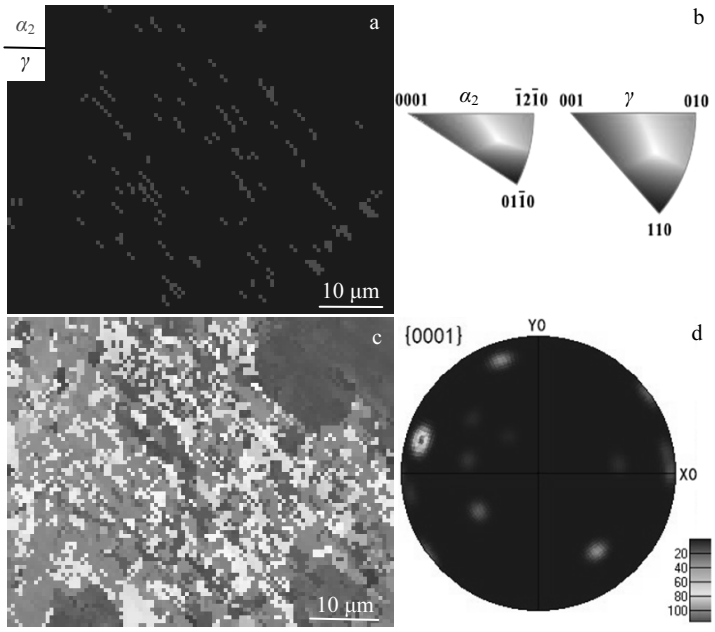

Fig.6 EBSD characterization of Ti-48Al-2Cr-2Nb alloy specimen formed by laser meting deposition: (a) EBSD phase diagram, (b, c) EBSD orientation map, and (d) $\alpha_2\{0001\}$ polar diagram

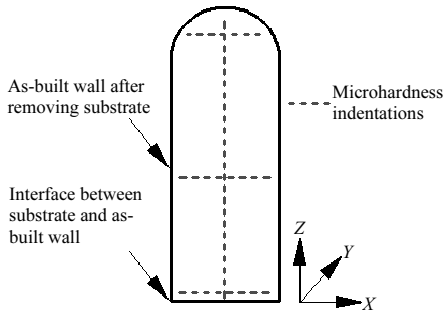

Fig.7 Diagram of Vickers hardness indentation of deposited sample

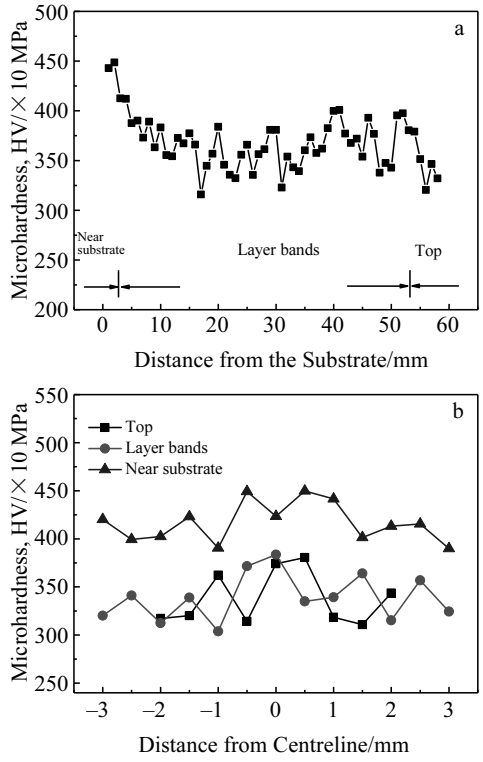

Fig.8 Microhardness distribution in cross section (*X*-*Z* plane): (a) along the direction of deposition (*Z* direction) and (b) along cross section *X* direction of top, middle and bottom

Biamino et al[16] have tested the mechanical properties of Ti-48Al-2Cr-2Nb materials. At room temperature, the tensile strength in *Z* direction is about 415 MPa. The room-temperature tensile strength of cast Ti-48Al-2Cr-2Nb alloy is 413 MPa. The elongation is 2.3%.

The measured results of mechanical properties of this experiment show that the tensile strength is 425 MPa and the elongation is 3.3%. From the results, it can be seen that the mechanical properties of Ti-48Al-2Cr-2Nb alloy fabricated by laser melting deposition are better than those of cast Ti-48Al-2Cr-2Nb alloy.

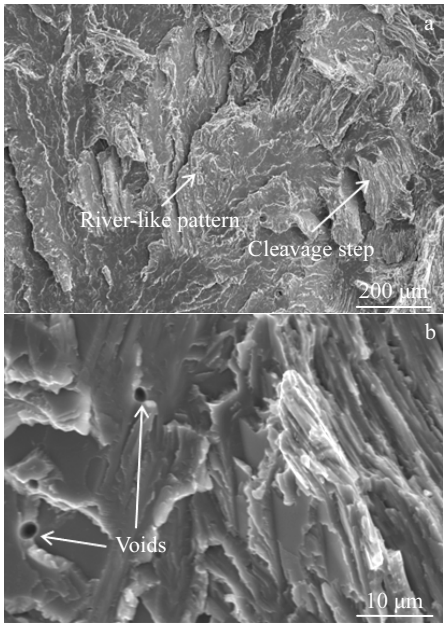

Fig.9 Morphologies of the fracture surface

The fracture morphology of tensile specimens is shown in Fig.9. From the figure, it can be seen that the fracture not only has a small cleavage step, but also has a certain plastic deformation, so it belongs to quasi-cleavage fracture.

3 Conclusions

1) Under the conditions of laser power 1400 W, scanning speed 9 mm/s, powder feeding speed 5.67 g/min and substrate preheating temperature 350 °C, 40 mm×5 mm×60 mm deposited sample are printed without surface cracks.

2) The microstructure of the deposited sample is composed of $\alpha_2+\gamma$ lamellar colony and a small amount of bulk γ phase. The content of γ and α_2 phase is 96.7% and 3.3%, respectively.

3) The average tensile strength in the deposited direction (*Z* direction) is 425 MPa, and the elongation is 3.3%. The tensile fracture morphology belongs to quasi-cleavage fracture. The hardness value near the substrate is about 4500 MPa, and the hardness value in other regions is about 3550 MPa.

References

1 Qu H P, Li P, Zhang S Q *et al*. *Materials & Design*[J], 2010, 31(4): 2201

2 Wang Qiang, Ding Hongsheng, Zhang Hailong *et al*. *Materials Characterization*[J], 2018, 137: 133

3 Karthikeyan S, Viswanathan G B, Gouma P I *et al*. *Materials Science and Engineering A*[J], 2002, 329-331: 621

4 Liang J M, Cao L, Xie Y H *et al*. *Materials Characterization*[J], 2019, 147: 116

5 Shang Chun. *Dissertation for Master*[D]. Shenyang: Shenyang Aerospace University, 2017 (in Chinese)

6 Jan Schwerdtfeger, Carolin Körner. *Intermetallics*[J], 2014, 49: 29
7 Qu H P, Li P, Zhang S Q *et al*. *Materials & Design*[J], 2010, 31(1): 574
8 Zhang X D, Brice C, Mahaffey D W *et al*. *Scripta Materialia*[J], 2001, 44(10): 2419
9 Zhang Yongzhong, Huang Can, Wu Fuyao *et al*. *Chinese Journal of Lasers*[J], 2010, 37(10): 2684 (in Chinese)
10 Qu H P, Wang H M. *Materials Science and Engineering A*[J], 2007, 466(1-2): 187
11 Li Wei, Liu Jie, Wen Shifeng *et al. Materials Characterization*[J], 2016, 113: 125
12 Li Wei, Liu Jie, Zhou Yan *et al*. *Intermetallics*[J], 2017, 85: 130
13 Li Wei, Liu Jie, Zhou Yan *et al. Scripta Materialia*[J], 2016, 118: 13
14 Zhang Kai, Wang Shijie, Liu Weijun *et al*. *Applied Surface Science*[J], 2014, 317: 839
15 Ma Yan, Cuiuri Dominic, Hoye Nicholas *et al*. *Materials Science and Engineering A*[J], 2015, 631: 230
16 Biamino S, Penna A, Ackelid U *et al*. *Intermetallics*[J], 2011, 19(6): 776

激光熔化沉积制造 γ-TiAl 合金的组织与性能

刘占起，王文博，马瑞鑫，徐国建，郑文涛
(沈阳工业大学，辽宁 沈阳 110870)

摘　要：通过激光熔化沉积制造技术制备了 *X*×*Y*×*Z*（40 mm×5 mm×60 mm）的 Ti-48Al-2Cr-2Nb 合金沉积样品。利用光学显微镜（OM）、扫描电子显微镜（SEM）、X 射线衍射（XRD）、透射电子显微镜（TEM）和电子背散射衍射（EBSD）分析了沉积样品的显微组织、相组成、晶粒取向及断口形貌；利用维氏硬度计测量了沉积样品不同位置的硬度分布；利用拉伸机测量了沉积样品在 *Z* 向的拉伸性能。结果表明，在最佳工艺参数条件下获得了成形良好的沉积样品，经过渗透检测后发现表面无裂纹。沉积样品的显微组织由 $\alpha_2+\gamma$ 层片状晶团及少量块状 γ-TiAl 相组成。在沉积状态下，沿试样 *Z* 方向的室温抗拉强度为 425 MPa，延伸率为 3.3%。拉伸试样的断口形貌为准解理断口。

关键词：激光熔化沉积；γ-TiAl 合金；显微组织；力学性能

作者简介：刘占起，男，1990 年生，博士，沈阳工业大学材料科学与工程学院，辽宁 沈阳 110870，电话：024-25496302，E-mail: 1640754283@qq.com